MADRID 2015
1-4 June 2015 | IFEMA Madrid

Tu N114 11

An Immersed Free Surface Boundary Treatment for Seismic Wave Simulation

L. Gao* (Univ. Grenoble Alpes), R. Brossier (Univ. Grenoble Alpes), B. Pajot (Bull/Atos, Grenoble), J. Tago (Universidad Nacional Autonoma de Mexico) & J. Virieux (Univ. Grenoble Alpes)

SUMMARY

Despite its popularity among the seismic community, finite difference method encounters difficulty for applications involving complex topography. Incorporating a free surface boundary treatment within the finite difference framework is appealing due to its efficiency and the effort-saving from existing finite difference codes. We present a free surface boundary treatment within the finite difference framework, with origin from the immersed boundary methods. Inherently, the presented boundary treatment is separated from the rest of the wave simulation, making it suitable for modularized code design. Specifically, we construct an extrapolation operator for each missing grid point to estimate its associated wavefield value at each time step. Although complicated in its mathematical expression, these operators only need to be constructed once for all time steps and source locations. Their associated memory consumption can be significant. Fortunately, simulating multiple shots together can dilute this memory cost. Application of these operators may incur numerical noise, leading to long time instability. In this case, additional numerical procedures such as introducing artificial diffusion are necessary to control the instability. The presented boundary treatment is shown to be capable of modeling both the body wave and surface wave accurately and has the potential on full waveform inversion applications.

Introduction

Finite difference method has been popular for wave simulation within the seismic exploration community, thanks to its efficiency. However, it encounters difficulty for applications involving complex topography, due to its regular grid pattern. Despite alternatives such as the spectral element method or the discontinuous Galerkin's method, incorporating the free surface boundary treatment within the finite difference framework is still appealing. Aside from efficiency, another motivation is the effort-saving from the legacy finite difference codes. We present such boundary treatment following the idea of the immersed boundary methods (Mittal and Iaccarino, 2005). The presented boundary treatment is naturally separated from the rest of the wave simulation, which makes it suitable for modularized code design and, therefore, easy to be incorporated in existing finite difference codes.

Methodology

We consider the stress-velocity formulation of the 2D isotropic elastic wave equation (1), where V_x and V_z stand for the velocity wavefields; σ_{xx}, σ_{xz} and σ_{zz} stand for the stress wavefields; ρ, λ and μ stand for the density and Lamé parameters. For simplicity, we omit the source terms at this stage.

$$\begin{cases} \dfrac{\partial V_x}{\partial t} &= \dfrac{1}{\rho}\dfrac{\partial \sigma_{xx}}{\partial x} + \dfrac{1}{\rho}\dfrac{\partial \sigma_{xz}}{\partial z}; \\ \dfrac{\partial V_z}{\partial t} &= \dfrac{1}{\rho}\dfrac{\partial \sigma_{xz}}{\partial x} + \dfrac{1}{\rho}\dfrac{\partial \sigma zz}{\partial z}; \\ \dfrac{\partial \sigma_{xx}}{\partial t} &= (\lambda+2\mu)\dfrac{\partial V_x}{\partial x} + \lambda\dfrac{\partial V_z}{\partial z}; \\ \dfrac{\partial \sigma_{xz}}{\partial t} &= \mu\dfrac{\partial V_z}{\partial x} + \mu\dfrac{\partial V_x}{\partial z}; \\ \dfrac{\partial \sigma_{zz}}{\partial t} &= \lambda\dfrac{\partial V_x}{\partial x} + (\lambda+2\mu)\dfrac{\partial V_z}{\partial z}. \end{cases} \quad (1)$$

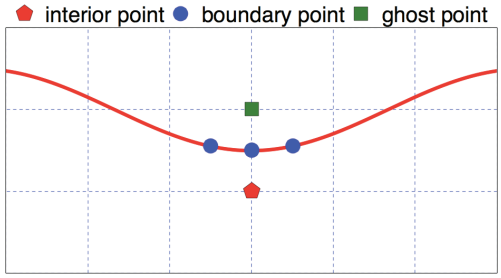

Figure 1 *Definition of the various types of points involved in the upcoming discussion.*

In addition to equation (1), the following boundary condition needs to be satisfied at the free surface:

$$\boldsymbol{\sigma} \cdot \vec{\mathbf{n}} = \mathbf{0}, \quad (2)$$

where $\boldsymbol{\sigma}$ stands for the stress tensor while $\vec{\mathbf{n}}$ stands for the normal direction. For flat free surfaces, a straightforward implementation of (2) is possible (Mittet, 2002). For non-trivial free surfaces, such as the one shown in Figure 1, one either needs to adapt the grid to conform to the free surface (Hestholm and Ruud, 1994), or to construct the wavefield values at the missing stencil points (Lombard et al., 2008). In this paper, we follow the second approach for its simplicity and portability. Specifically, we construct the wavefield values at the ghost points at each time step. The definition of a ghost point is illustrated in Figure 1, along with boundary point and interior point. This construction process has to respect both the continuity of the wavefields and the free surface boundary condition (2). Conceptually, we can split this construction process into two stages. In the first stage, we extrapolate the wavefields from the interior points to the boundary points, during which we impose the free surface boundary condition. In the second stage, we further extrapolate the wavefields from the boundary points to the ghost points.

The first extrapolation can be formulated as a linear equality constrained least squares (LSE) problem. To derive the LSE problem, we start from the Taylor expansion of function f from boundary point (x_b, z_b) to one of its nearby interior points (x_i, z_i). For instance, truncated at the second order, we have:

$$\begin{aligned} f(x_i,z_i) &= f(x_b,z_b) + \Delta x_i \frac{\partial f}{\partial x}(x_b,z_b) + \Delta z_i \frac{\partial f}{\partial z}(x_b,z_b) \\ &+ \frac{1}{2!}\left((\Delta x_i)^2 \frac{\partial^2 f}{\partial x^2}(x_b,z_b) + 2\Delta x_i \Delta z_i \frac{\partial^2 f}{\partial x \partial z}(x_b,z_b) + (\Delta z_i)^2 \frac{\partial^2 f}{\partial z^2}(x_b,z_b) \right) + \mathscr{O}(h^3), \end{aligned} \quad (3)$$

where $\Delta x_i = x_i - x_b$, $\Delta z_i = z_i - z_b$, $h = \max(\Delta x_i, \Delta z_i)$ and f denotes any of the wavefields. To determine

the values of f, $\frac{\partial f}{\partial x}$, $\frac{\partial f}{\partial z}$, $\frac{\partial^2 f}{\partial x^2}$, $\frac{\partial^2 f}{\partial x \partial z}$ and $\frac{\partial^2 f}{\partial z^2}$ at (x_b, z_b) from the values of various $f(x_i, z_i)$, we can formulate a least squares problem, which leads to results that satisfy the continuity of the wavefields well.

We define column vector $u = \left[f, \frac{\partial f}{\partial x}, \frac{\partial f}{\partial z}, \frac{\partial^2 f}{\partial x^2}, \frac{\partial^2 f}{\partial x \partial z}, \frac{\partial^2 f}{\partial z^2}\right]^T$, evaluated at (x_b, z_b). Suppose m interior points near (x_b, z_b) are invoked for its extrapolation, denoted as (x_1, z_1), (x_2, z_2), $\cdots$, (x_m, z_m), correspondingly. We define column vector b such that $b_i = f(x_i, z_i)$ for $i = 1, \ldots, m$. Moreover, we define A as the matrix whose component at the ith row and jth column is the Taylor expansion coefficient corresponding to u_j for interior point (x_i, z_i). We can now put the Taylor expansion for all the m nearby interior points into a succinct matrix form: $b = Au + e$, where e denotes the residual vector. To determine u, we can use the minimization problem: $u = \arg\min_v \|Av - b\|_2^2$. Its generalization from a scalar f to a vector $\mathbf{f}$ is straightforward. We only need to stack together u, b and A corresponding to each component of $\mathbf{f}$ to obtain the minimization problem for $\mathbf{f}$, as shown in (4). Consequently, matrix $\mathbf{A}$ is block diagonal.

$$\mathbf{u} = \arg\min_{\mathbf{v}} \|\mathbf{A}\mathbf{v} - \mathbf{b}\|_2^2. \tag{4}$$

However, the smooth extension of $\mathbf{f}$ obtained from (4) does not necessarily satisfy the free surface boundary condition (2). To address this issue, we can impose (2) as constraints for (4). Moreover, since the derivatives of $\mathbf{f}$ are also listed as unknowns in (4), we can include derivatives of the free surface boundary condition as constraints for (4) as well. We denote these constraints, in a succinct matrix form, as: $\mathbf{C}\mathbf{u} = \mathbf{d}$. Combining with the minimization problem (4), we arrive at the following LSE problem:

$$\begin{aligned} \mathbf{u} \quad = \quad & \arg\min_{\mathbf{v}} \|\mathbf{A}\mathbf{v} - \mathbf{b}\|_2^2 \\ & s.t. \;\; \mathbf{C}\mathbf{v} = \mathbf{d}. \end{aligned} \tag{5}$$

With the outputs from (5), the second stage of the construction process, i.e., extrapolation from the boundary points to the ghost points, can be achieved straightforwardly by Taylor expansion. Practically, we associate each ghost point with several nearby boundary points and use the averaged Taylor expansion results as the extrapolated wavefields. We note that the implementations of source terms and PML layers do not interfere with the presented free surface boundary treatment. Moreover, the presented free surface boundary treatment can be viewed as an add-on to the underlying wave simulation algorithm.

The presented two extrapolations can be combined to construct an extrapolator that is invariant to different time steps while links the ghost point directly with the nearby interior points. By doing so, we avoid solving the LSE problem at each time step. Consequently, the floating point operations needed for the free surface boundary treatment is comparable with the wavefield simulation. However, the memory consumption associated with the boundary treatment can still be significant. Nevertheless, we can dilute the memory cost via simulating multiple shots together with domain decomposition parallelism.

In practice, we encounter long time instability with the presented free surface boundary treatment in our implementation. Specifically, we use second-order staggered grid finite difference scheme (Virieux, 1986) and leapfrog scheme for the wavefield simulation. Currently, we adopt a rudimentary but pragmatic strategy to counterbalance the instability, that is to add artificial diffusion (Virieux and Madariaga, 1982). Namely, we append the Laplacian terms $\alpha \Delta V_x$ and $\alpha \Delta V_z$ to the first two equations in (1), respectively, where α is a tunable parameter that controls the amount of diffusion. On-the-fly filtering will be investigated in the future as a more delicate alternative to control the instability. Since we only need to add diffusion at the nearby region of the free surface, the additional computational cost is insignificant.

Numerical Examples

We present several numerical examples to demonstrate the behavior of the presented free surface boundary treatment. Isotropic elastic wave equation in 2D or 3D with homogeneous media is considered in the following.

Example 1: Garvin's problem

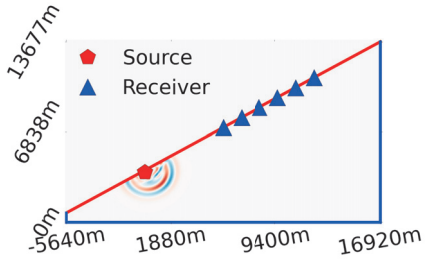

Figure 2 *Geometric configuration.*

A quadrilateral domain as shown in Figure 2 is considered. The angle between the free (top) surface and the horizontal line is roughly 30°. PML layers are appended at the other three edges. P- and S-wave velocities are specified as $5640m/s$ and $2870m/s$, respectively. Ricker wavelet with peak frequency 5Hz is used as the explosive source. The underlying grid size leads to roughly 16.3 points per wavelength for the minimal shear wavelength, corresponding to 12.5Hz frequency.

The seismograms corresponding to the source and receiver locations, as depicted in Figure 2, are shown in Figure 3, in comparison with the analytic solution. We observe good agreements in Figure 3 despite loss of amplitude in the surface wave, due to the side effect of artificial diffusion.

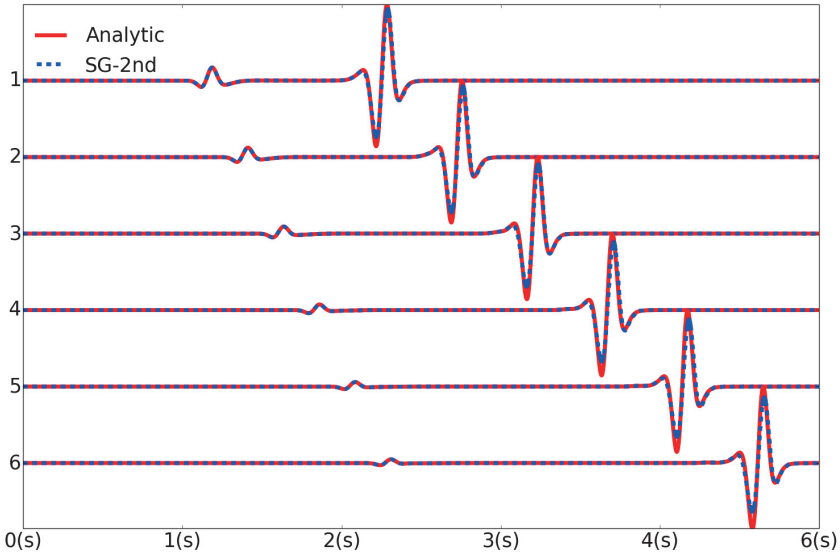

Figure 3 *Seismograms.*

	EM	PM	$D_{SR}(\lambda)$
R1	9.1E-02	3.4E-02	28.6
R2	1.1E-01	4.1E-02	35.2
R3	1.3E-01	4.7E-02	41.8
R4	1.4E-01	5.5E-02	48.4
R5	1.6E-01	6.1E-02	55.0
R6	1.7E-01	6.7E-02	61.6

Table 1 *Misfit quantification (Kristeková et al., 2006) corresponding to Figure 3. 'R' stands for Receiver, 'EM' stands for Envelop Misfit, 'PM' stands for Phase Misfit, D_{SR} denotes the source receiver (linear) distance and λ denotes the minimal shear wavelength.*

Example 2: Sinusoidal free surface

A sinusoidal free surface with $705m$ amplitude is considered in this example. Numerical parameters are the same as in Example 1. The simulated seismograms are shown in Figure 4, demonstrating good agreements with the DG solution (Tago et al., 2012). The misfit quantification is shown in Table 2.

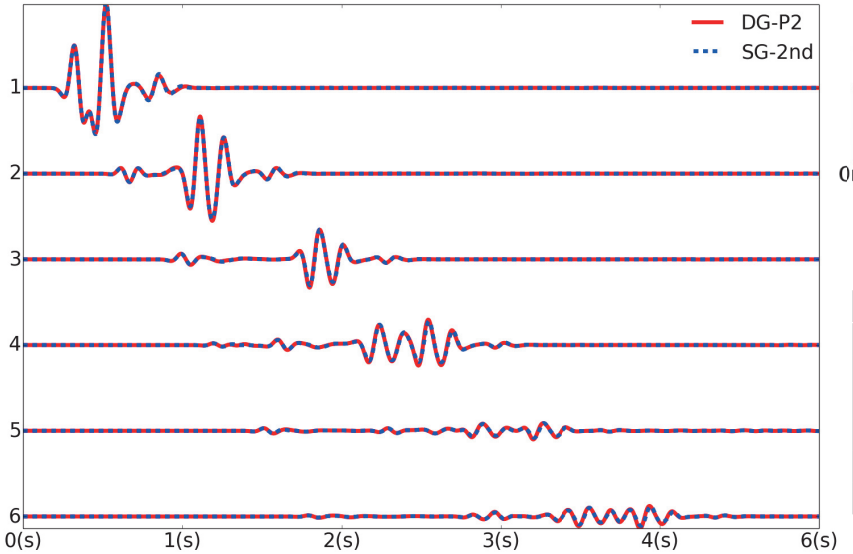

Figure 4 *Seismograms.*

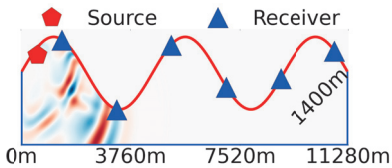

	EM	PM	$D_{SR}(\lambda)$
R1	2.2E-02	3.9E-03	3.8
R2	2.5E-02	8.0E-03	12.7
R3	5.9E-02	2.4E-02	20.0
R4	1.1E-01	4.3E-02	28.3
R5	1.7E-01	6.6E-02	36.4
R6	2.0E-01	8.9E-02	44.5

Table 2 *Misfit quantification.*

Example 3: Tilt plane free surface in 3D

A 3D domain is considered in this example with the free surface tilted for 11° on x-direction and kept horizontal on y-direction. Numerical parameters are the same as in Example 1. The simulated seismograms are shown in Figure 6, demonstrating good agreements with the DG solution. The source receiver distance is 3.0λ, 6.1λ, 9.2λ, 12.4λ, 15.5λ, 18.6λ for receivers 1 to 6, correspondingly. The misfit quantification is shown in Table 3.

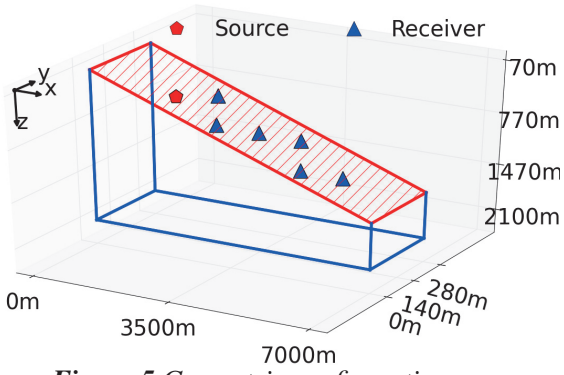

Figure 5 *Geometric configuration.*

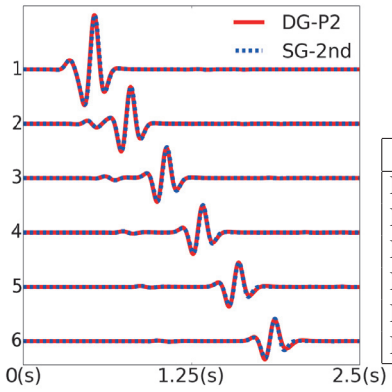

Figure 6 *Seismograms.*

	EM	PM
R1	1.2E-02	3.2E-02
R2	1.9E-02	3.3E-02
R3	2.4E-02	3.5E-02
R4	3.5E-02	3.0E-02
R5	5.6E-02	2.1E-02
R6	6.8E-02	1.3E-02

Table 3 *Misfit.*

Conclusions

A boundary treatment for non-trivial free surface is presented for seismic wave simulation within the finite difference framework. Well-defined mathematical abstraction and numerical examples are demonstrated. Belonging to the family of the immersed boundary methods, the presented boundary treatment is naturally separated from the rest of the wave simulation, thus can be absorbed by the existing codes. Despite extra computational cost, the presented boundary treatment is shown to possess potential on the full waveform inversion applications.

Acknowledgements

This study was partially funded by the SEISCOPE consortium (*http://seiscope2.osug.fr*), sponsored by BP, CGG, CHEVRON, EXXON-MOBIL, JGI, PETROBRAS, SAUDI ARAMCO, SCHLUMBERGER, SHELL, SINOPEC, STATOIL, TOTAL and WOODSIDE. This study was granted access to the HPC resources of CIMENT infrastructure (https://ciment.ujf-grenoble.fr) and CINES/IDRIS under the allocation 046091 made by GENCI.

References

Hestholm, S. and Ruud, B. [1994] 2d finite-difference elastic wave modelling including surface topography. *Geophysical Prospecting*, **42**(5), 371–390.

Kristeková, M., Kristek, J., Moczo, P. and Day, S.M. [2006] Misfit criteria for quantitative comparison of seismograms. *Bulletin of the seismological Society of America*, **96**(5), 1836–1850.

Lombard, B., Piraux, J., Gelis, C. and Virieux, J. [2008] Free and smooth boundaries in 2-D finite-difference schemes for transient elastic waves. *Geophysical Journal International*, **172**, 252–261.

Mittal, R. and Iaccarino, G. [2005] Immersed boundary methods. *Annual Review of Fluid Mechanics*, **37**, 239–261.

Mittet, R. [2002] Free-surface boundary conditions for elastic staggered-grid modeling schemes. *Geophysics*, **67**(5), 1616–1623.

Tago, J., Cruz-Atienza, V.M., Virieux, J., Etienne, V. and Sánchez-Sesma, F.J. [2012] A 3d hp-adaptive discontinuous galerkin method for modeling earthquake dynamics. *Journal of Geophysical Research: Solid Earth (1978–2012)*, **117**(B9).

Virieux, J. [1986] P-SV wave propagation in heterogeneous media, velocity-stress finite difference method. *Geophysics*, **51**, 889–901.

Virieux, J. and Madariaga, R. [1982] Dynamic faulting studied by a finite difference method. *Bulletin of the Seismological Society of America*, **72**, 345–369.